Engineering Structures 284 (2023) 115924

Contents lists available at ScienceDirect

Engineering Structures

journal homepage: www.elsevier.com/locate/engstruct

Bayesian structural parameter identification from ambient vibration in cultural heritage buildings: The case of the San Jerónimo monastery in Granada, Spain

Enrique Hernández-Montes [a], María L. Jalón [a,*], Rubén Rodríguez-Romero [c], Juan Chiachío [a,b], Víctor Compán-Cardiel [c], Luisa María Gil-Martín [a]

[a] Department of Structural Mechanics and Hydraulic Engineering, University of Granada, Spain
[b] Andalusian Research Institute in Data Science and Computational Intelligence (DaSCI), Granada, Spain
[c] Department of Building and Ground Engineering, University of Seville, Spain

ARTICLE INFO

Keywords:
Ambient vibration tests
Bayesian learning
Cultural heritage buildings
Finite element models
Operational modal analysis

ABSTRACT

The deterioration of Cultural Heritage assets caused by the natural hazards is a pressing issue in many countries. Therefore, reliable models based on the large-scale structural response of the assets is key to assess their resilience. However, reliable models such as large and detailed Finite Element (FE) models, require a large number of data and input parameters. This paper proposes a Bayesian learning approach to identify the main parameters of a FE model with quantified uncertainty based on ambient vibration data. As a novelty when compared with other Bayesian structural parameter identification methods from ambient vibration data, here the likelihood function is formulated in a principled way considering information from both frequencies and modes using a probabilistic version of the Modal Assurance Criterion for the modes. This method is embedded into a parameterised computational model to automate the simulation process, and a real case study for a sixteenth century heritage building in Granada (Spain) is presented. The results show the suitability and effectiveness of the proposed Bayesian approach in identifying the most plausible values of the uncertain model parameters in a rigorous probabilistic way, but also in obtaining the modelled frequencies and the modal assurance criterion values with quantified uncertainty.

1. Introduction

The fire at the Notre-Dame Cathedral in 2019 brought to light the importance of cultural heritage preservation. A prospective resilience assessment of such cultural heritage (CH) sites and buildings is the foundation upon which an efficient knowledge-based preservation will be based. In particular, structural integrity against natural hazards, such as climate-related loads (snow, wind, etc.), geo-hazards (e.g., earthquakes) and man-made hazards (e.g., fires), play a critical role in the overall CH asset resilience assessment. Analysing the effects of such hazards on a building with the precision required means that *reliable models* of the building are needed. These reliable models are based on information from the structure response coming from measured data, process known as the inverse problem [1]. One of the most commonly encountered inverse problems in structural engineering is the identification of uncertain model parameters (e.g., the effective stiffness) based on information from the vibration signature of the structure. Most of the authors propose deterministic approaches for the inverse problem of model parameter identification using experimental modal data from Ambient Vibration Tests (AVTs). Examples can be found in [2] in application to the Cathedral of Santiago (Chile), in [3–6] applied to several historical Italian palaces and towers, or in [7] in application to various Iranian mosques. However, deterministic inverse problem approaches do not account for the uncertainty coming from measurement errors and, above all, from the fact that the model itself is a idealisation of reality and has a limited correspondence with reality. Consequently, probabilistic instead of deterministic approaches for the inverse problem are preferred to deal with these sources of epistemic uncertainty. In this context, the Bayesian inverse problem methodology [8,9] provides a rigorous yet efficient framework for model parameter identification (updating) while accounting for the associated uncertainties.

The Bayesian inverse problem of parameter identification based on experimental modal data from ambient vibration tests is widely known and it has been shown to be efficient when applied to linear structures, bridges or buildings. For example, Cheung and Bansal [10] proposed a

* Corresponding author.
E-mail address: mljalon@ugr.es (M.L. Jalón).

https://doi.org/10.1016/j.engstruct.2023.115924
Received 28 June 2022; Received in revised form 3 February 2023; Accepted 28 February 2023
Available online 20 March 2023

new algorithm for Bayesian system identification of a linear structural model based on incomplete modal data, considering the modal shapes as uncertain variables. Jang and Smyth [11] developed a Bayesian model updating framework for a full-scale bridge FE model, using the natural frequencies and the mode shapes residual vectors in the error function of the likelihood function. Chiara et al. [12] proposed a Bayesian model parameter identification framework for a curved cable-stayed footbridge using the natural frequencies as reference data for the model updating, whereas the modal shapes were considered as constraints in the computation of the likelihood function to ensure mode shape matching.

In application to building structures, Lam et al. [13] proposed an enhanced simulation algorithm for the Bayesian model updating of a coupled-slab system using measured modal data. Ierimonti et al. [14] investigated the calibration of a base-isolated building FE model using natural frequencies and continuous monitoring through a continuous Bayesian model updating. Akhlaghi et al. [15] identified surface damage in a building proposing a Bayesian inference process to combine natural frequencies and point cloud data. Liu et al. [16] proposed a Bayesian model updating method using subset simulation optimisation given ambient vibration data to improve the sampling efficiency, and applied such a methodology in a full-scale high-rise structure.

In the context of historical masonry buildings, a few authors have investigated the suitability of the Bayesian framework to update the relevant mechanical and structural parameters of this type of structures. For example, Atamturktur et al. [17], applied the Bayesian methodology to update FE models of masonry choir vaults. More recently, Monchetti et al. [18] have carried out a Bayesian updating of the FE model parameters of a masonry tower. Both research works do not consider the mode shapes in the model updating procedure, using the natural frequencies as the only system output, thus neglecting a useful piece of information which is available in the data. Besides, to the best of the authors' knowledge, the suitability of the Bayesian methodology has not been explored so far in application to a complete CH stone masonry building. These are distributed mass structures full of complex structural elements such as buttresses, domes, and towers. There were built of natural materials such as stone, rammed earth, wood, among others, whose structural properties are uncertain. Quantifying such uncertainty in the specific case of degraded historical buildings is key for rigorous and complete structural parameter identification; this is precisely the context where the full potential of the probabilistic Bayesian approach for parameter identification can be fully exploited.

In this paper, a rational methodology for structural parameter identification of CH buildings based on the Bayesian learning approach is presented. First, experimental data about modal parameters (natural frequencies and mode shapes) from Ambient Vibration Tests (AVTs) are collected, which have been obtained using Operational Modal Analysis (OMA) algorithms. Next, a complete building model is developed using geometrical 3D data coming from a 3D laser scanner, which is used to develop a simplified but reliable structural FE model of the entire building. Several structural parameters of the FE model are uncertain, so a Bayesian inverse problem using modal data (both frequencies and modes) is finally adopted to infer the most plausible values of these parameters.

As a novelty when compared with other Bayesian structural parameter identification approaches from AVTs data, here the *likelihood function* is formulated in a principled way considering information from both frequencies and mode shapes, using a probabilistic version of the Modal Assurance Criterion (MAC) for the mode shapes. By means of this, and in contrast to other existing methods, the proposed approach does not require the matching of measured modes with the corresponding modes from the FE model, which greatly simplifies the identification procedure. The proposed methodology is generic but here it has been specialised using a real case study for a sixteenth century CH building in Granada (Spain). The results show the efficiency of the proposed methodology in identifying the most plausible values of the main mechanical and material parameters of the building based on modal data in a rigorous probabilistic way.

The remainder of the paper is organised as follows: Section 2 describes the geometry of the CH building proposed. Section 3 describes the methodology used to update structural FE models of CH buildings. In Section 4, the proposed methodology is illustrated and tested for the San Jerónimo Monastery. Section 5 discusses the main results and lessons learned. Section 6 provides the conclusions and future works that can be derived from this research.

2. Geometrical description of the CH asset

The San Jerónimo Monastery in Granada (Spain) is a sixteenth century CH building located in the city centre. The CH building was built in the Renaissance architectural style, and it has two excellent cloisters as well as the church and the bell tower (Fig. 1(a)). The main cloister is a large square enclosing a central garden of orange trees, and it is surrounded by two floors of side galleries, each with nine arches. The church, has a latin cross plan with an spectacular elevated choir at its entrance of the church and an extraordinary altarpiece behind a wide staircase, whose floor dimension is 57 × 24 m, and the height of the central nave is 30 m and the dome is 35 m high. The bell tower is located on the main facade with 46 m of height (Fig. 1(b)). The monastery was plundered during 19th century and was converted into cavalry barracks, which almost led to the ruin of the architectural complex. The State undertook a complete restoration of the building in 1916–1920, and there have been other small-scale restoration works since then.

The structural system consists of stone masonry walls (walled-structure) with exterior buttresses. The main construction material is limestone, quarried in the Santa Pudia area (15 km from Granada) which was commonly used in the CH buildings of the city as a construction material (for example: the Cathedral, the Palace of Carlos V, the Royal Hospital, or the Green Bridge). Santa Pudia limestone is quite porous and highly susceptible to traffic pollution and severe climates, such as that of Granada, which is characterised by major daily and seasonal thermal oscillations, with very low minimum and very high maximum temperatures in the winter and in the summer, respectively [19,20]. However, other construction materials also appear in the building. Concrete appears on the top two floors of the bell tower as this was used during its reconstruction, wooden trusses also appear as part of the roof structure, and handmade bricks [21–23] are used in the cannon vault.

In order to model all the structural and non-structural details of the monastery, a 3D RIEGL LMS-Z420i [24] laser scanner is used as a novel non-destructive technology for deriving the point clouds for the interior and the exterior of the monastery. The point clouds obtained from different scans are processed and synchronised using RISCAN PRO software. After the synchronisation and combination of point clouds, the 3D model of the structure is constructed using the Agisoft Metashape [25] software package. The resulting geometrical 3D data for the exterior of the monastery, the church and the roof support are presented in Fig. 2.

3. Bayesian inverse problem

3.1. Forward problem: FE modelling

The geometrical 3D data obtained from the point cloud explained in Section 2 are used to develop a structural FE model of the building using ANSYS. The model is conceived in a way that is computationally affordable in the context of a probabilistic inverse problem, where thousands of forward model simulations are needed, but it is also reliable enough to capture the main modal response of the building. This simplified FE model is based on the 3D macro-modelling technique, which has

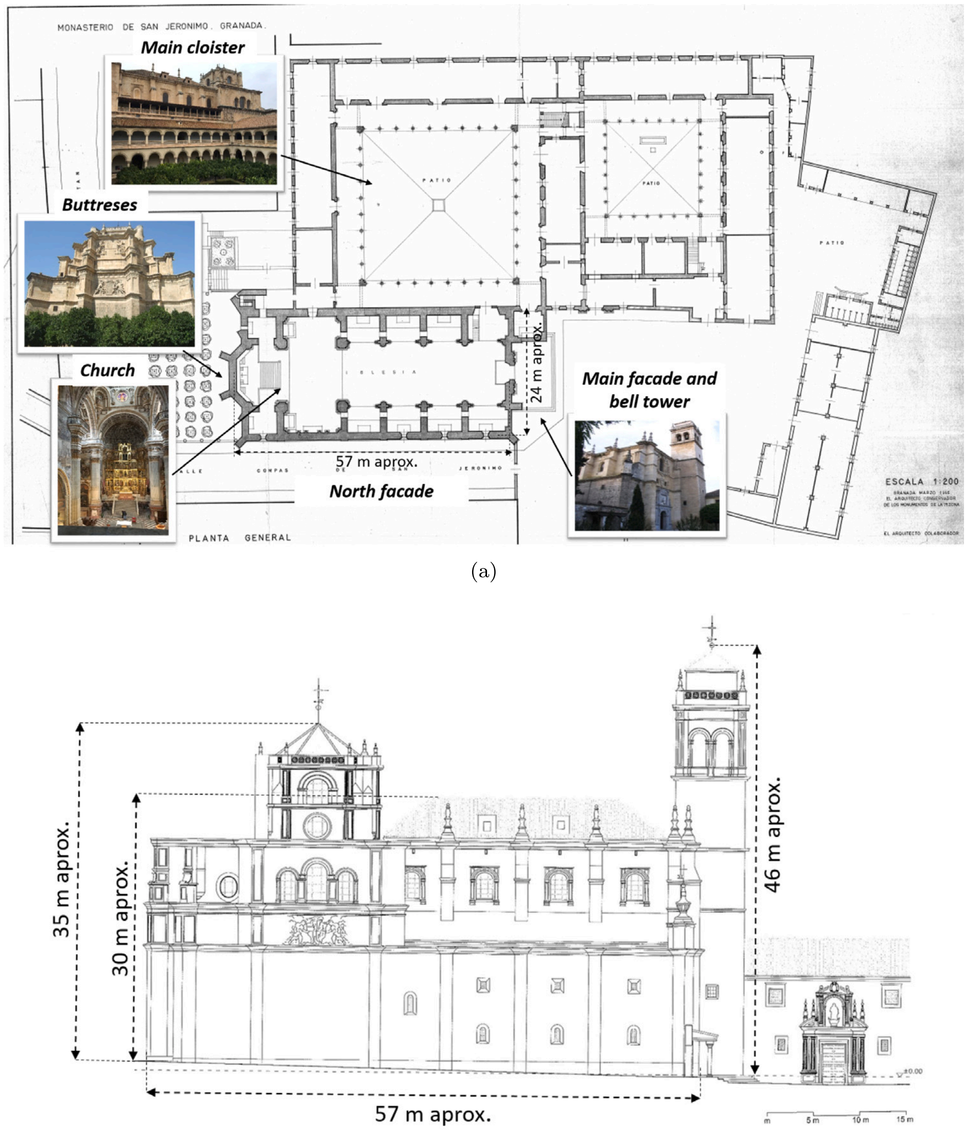

(a)

(b)

Fig. 1. Views of San Jerónimo Monastery. (a) Plan view, (b) Elevation view of the north facade.

been shown to be efficient when applied to masonry constructions [26–29]. In this sense, the material components modelled (bricks, stone, and concrete and their contact interfaces) are considered as homogeneous and isotropic materials.

Shell-type elements (SHELL181) are used with six degrees of freedom at each node, considering both bending and membrane stiffness, with just one element through thickness to avoid unnecessary model complexity. The main cloister is adjacent to the church (see Fig. 1(a)) and this boundary condition is modelled by vertical walls using SHELL181 elements. In addition, the inner arcade of the church, on which the canon vault rests lengthwise, has been modelled as a solid wall, and this process also uses SHELL181.

In order to consider the influence of foundation soil stiffness in the modal response of the building, the Winkler elastic foundation theory is adopted [30]. The soil–structure interaction is idealised with a set of springs with no interaction between them, and a linear stress–strain behaviour is assumed leading to simple simulations. This spring model only needs the modulus of sub-grade reaction as parameter to represent the soil, so nonlinearities are neglected. Springs are represented by COMBIN14 elements in the foundation level of the FE model. The COMBIN14 elements are 3-D uniaxial longitudinal spring–dampers with no mass, widely used in the soil–structure model interaction [31]. These elements have damping capabilities, however only the longitudinal spring constant is considered in this study.

In regards to the mesh size, it is appropriately tuned after a mesh convergence study (not shown here for the sake of conciseness) in such a way that the FE model outputs become independent of the mesh size. Specifically, 1.25 m^2 and 1 m are used in this research as the average surface of the SHELL181 elements and the average length of the COMBIN14 elements, respectively. Fig. 3 illustrates the structural FE model of the CH building with indication of the boundary conditions.

Finally, the described FE model is parameterised considering several mechanical and material parameters as uncertain input model parameters such as the bulk modulus of the main construction material (E), the bulk modulus of the main cloister walls (E_c), the bulk modulus of the inner arcade of the church (E_a), and the stiffness of the soil (k). Such parameters were revealed as ‘sensitive’ after a Global Sensitivity Analysis of the FE model [32].

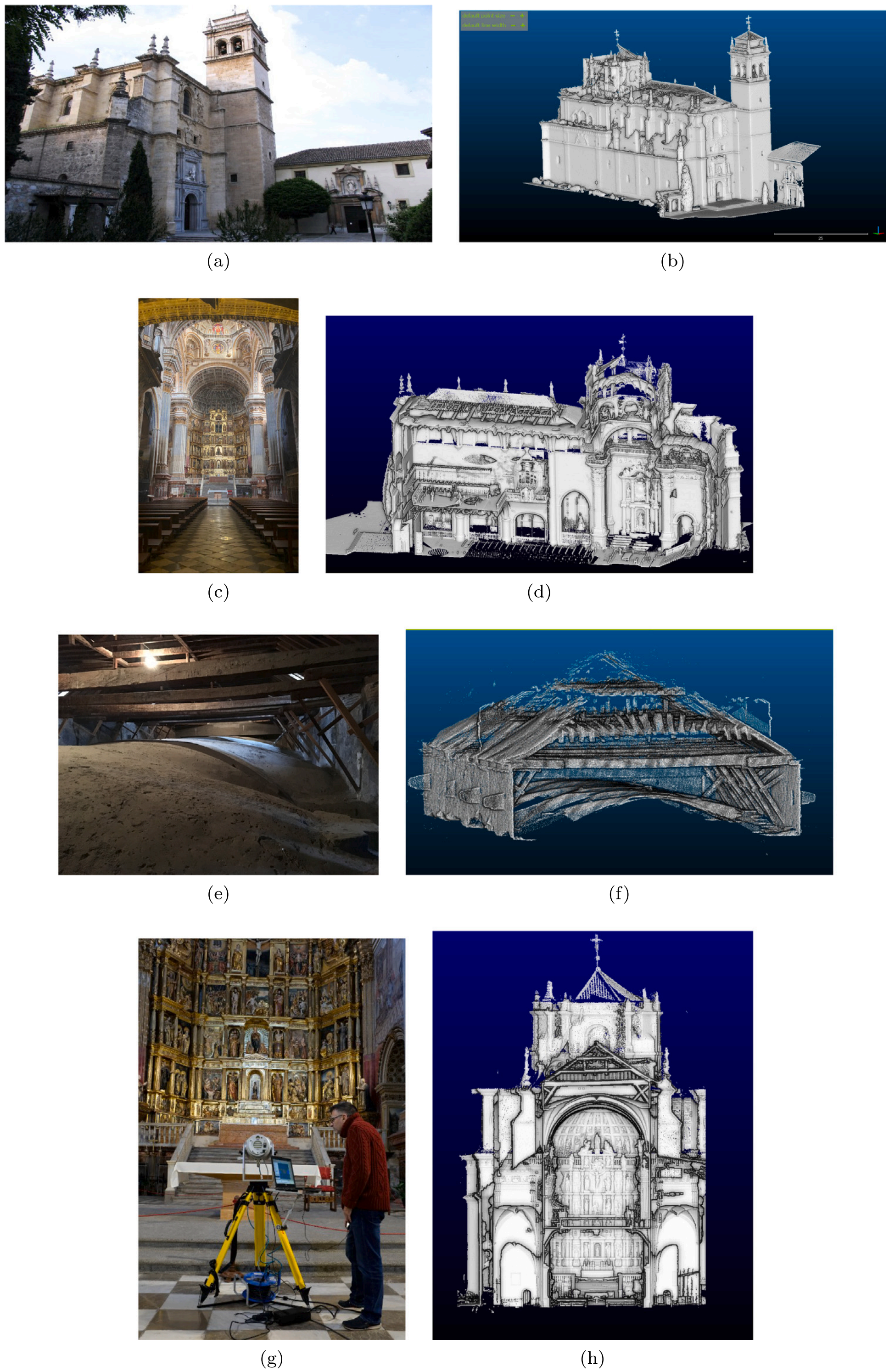

Fig. 2. Geometrical 3D data: (a) image of the exterior, (b) point cloud of the exterior, (c) image of the interior, (d) point cloud of the interior, (e) image of the roof's support (f) point cloud of roof's support, (g) image of altar piece, (h) point cloud of the altar piece.

3.2. Bayesian model parameter identification

The FE model proposed in Section 3.1 is based on a set of modelling assumptions and simplifications to decrease computational complexity. Estimating a deterministic single value for the unknown model parameters using such a model has limited meaning if the model itself is considered as an idealisation of reality, and furthermore, if the numerical and measurement errors exist. In order to provide a reliable estimation, probabilistic instead of deterministic values for model parameters should be provided, which give information about the *degree of belief* of the estimated model parameters that provide the (noisy) observations of the system response. The Bayesian inverse problem is a principled and rigorous way to tackle such sources of uncertainty in the parameter estimation [9].

Within the Bayesian Inverse Problem (BIP) [9], the interest is to obtain the *posterior* plausibility of the values of uncertain parameters $\boldsymbol{\theta} = \{\theta_1, \theta_2, \ldots, \theta_n\}$ given the measured system response, $\mathcal{D}$, for a specific model class, $\mathcal{M}$, that idealises the physical system. This is represented

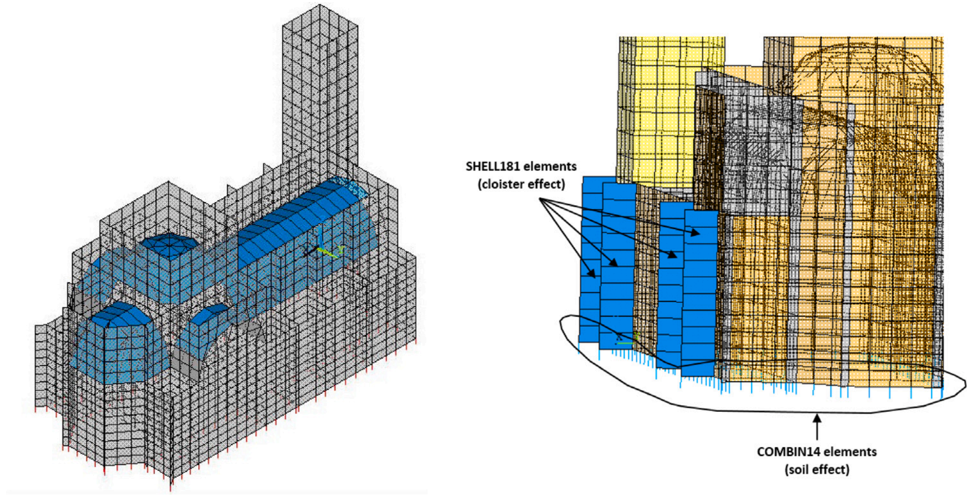

Fig. 3. Structural FE model of San Jerónimo Monastery (Granada, Spain): (a) mesh details, (b) boundary conditions details.

by PDF $p(\theta|\mathcal{D},\mathcal{M})$, which is obtained using Bayes' theorem as follows:

$$p(\theta|\mathcal{D},\mathcal{M}) = c^{-1} p(\mathcal{D}|\theta,\mathcal{M}) p(\theta|\mathcal{M}) \tag{1}$$

with c as a normalising constant so that $p(\theta|\mathcal{D},\mathcal{M})$ represents a valid PDF, i.e., $\int p(\theta|\mathcal{D},\mathcal{M}) = 1$. Note that Bayes' theorem takes the initial degree of belief of model parameters θ for the given model, $\mathcal{M}$, which is expressed by the *prior* PDF $p(\theta|\mathcal{M})$, and *updates* this plausibility to obtain the *posterior* degree of belief of the parameters by using information from the system response (both model and data) expressed through PDF $p(\mathcal{D}|\theta,\mathcal{M})$, known as the *likelihood function*. The likelihood function provides a measurement about how likely observed data $\mathcal{D}$ are reproduced by a model specified by θ if model class $\mathcal{M}$ is adopted. Note that there is not any invocation of randomness in Eq. (1). Rather, the probability is interpreted here as a multi-valued logic that expresses the relative plausibility of the values of the model parameters conditioned to a given model specified by $\mathcal{M}$. This interpretation of probability is not well known in engineering, where there is a widespread belief that probability only applies to aleatory uncertainty (i.e., inherent randomness) and not to epistemic uncertainty (degree of belief).

3.2.1. Description of the prior plausibility of model parameters

The prior PDF of model parameters $p(\theta|\mathcal{M})$ is defined as the unconditional product of the individual parameters, i.e., $p(\theta|\mathcal{M}) = \prod_i p(\theta_i|\mathcal{M})$. Note that this is not an assertion that no correlations actually exist in model parameters, it is only a description of our prior knowledge about such correlations. If they existed, they would become apparent after Bayesian updating and therefore, they would be considered in the forward model simulations. The Principle of Maximum Information Entropy (PMIE) [33] is conservatively adopted to assign a probability model for individual model parameters $p(\theta_i|\mathcal{M})$ so that it produces the largest uncertainty (largest Shannon entropy). According to PMIE, the maximum-entropy model for an unrestricted parameter with a known mean of μ_{θ_i} and a variance of σ_{θ_i} is the Gaussian PDF, i.e., $p(\theta_i|\mathcal{M}) = \mathcal{N}(\mu_{\theta_i}, \sigma_{\theta_i})$; for an interval bounded parameter $\theta_j \in [a,b]$, the maximum-entropy model is the uniform distribution $p(\theta_j|\mathcal{M}) = \mathcal{U}(a,b)$. Depending on our prior knowledge about the individual model parameters, either uniform or Gaussian probability models can be adopted as appropriate. Further information about the prior probability models adopted for model parameters is provided in Section 4.

3.2.2. Likelihood function definition

As stated earlier, the likelihood function is obtained as the plausibility of data $\mathcal{D}$ being reproduced by model $\mathcal{M}$ specified by θ. In this study, the data corresponds to the frequencies measured $\{\hat{f}_1, \hat{f}_2, \ldots, \hat{f}_N\}$ and modes $\{\hat{\phi}_1, \hat{\phi}_2, \ldots, \hat{\phi}_N\}$ of the building, i.e., $\mathcal{D} = \{\hat{\mathbf{y}}_1, \hat{\mathbf{y}}_2, \ldots, \hat{\mathbf{y}}_N\}$, with $\hat{\mathbf{y}}_i = (\hat{f}_i, \hat{\phi}_i)$. Therefore, $p(\mathcal{D}|\theta,\mathcal{M}) = \prod_i^N p(\hat{\mathbf{y}}_i|\theta,\mathcal{M})$ with $p(\hat{\mathbf{y}}_i|\theta,\mathcal{M}) \equiv p(\mathbf{g}_i(\theta) = \hat{\mathbf{y}}_i|\theta,\mathcal{M})$. Assuming stochastic independence between the likelihood of frequencies and modes, $p(\hat{\mathbf{y}}_i|\theta,\mathcal{M})$ for the ith vibration mode can be formulated as the unconditional product of probabilities $p(\hat{f}_i|\theta,\mathcal{M})$ and $p(\hat{\phi}_i|\theta,\mathcal{M})$, as

$$p(\hat{\mathbf{y}}_i|\theta,\mathcal{M}) = p(\hat{f}_i|\theta,\mathcal{M}) p(\hat{\phi}_i|\theta,\mathcal{M}) \tag{2}$$

It should be highlighted that the stochastic independence shown in Eq. (2) refers to *information independence* and should not be confused with *causal independence*. It is equivalent to asserting that if our information about frequencies is 'good' (e.g., large likelihood $p(\hat{f}_i|\theta,\mathcal{M})$), this does not necessarily means that the information about modes must be equally good.

In Eq. (2), the frequency component $p(\hat{f}_i|\theta,\mathcal{M})$ can be obtained by defining a discrepancy function between the measured and modelled frequencies as $J_f(\theta) = \hat{f}_i - f_i(\theta)$, and $f_i(\theta)$ is the ith frequency that is reproduced by the FE model specified by θ. Since θ are uncertain variables, so is $J(\theta)$; according to PMIE, $J(\theta)$ can be conservatively assumed to follow a Gaussian white noise (zero-mean) process for different θ values, i.e., $J(\theta) \sim \mathcal{N}(0,\sigma_f)$, therefore,

$$J_f(\theta) = \hat{f}_i - f_i(\theta) \sim \mathcal{N}(0,\sigma_f) \implies \hat{f}_i \sim \mathcal{N}(f_i(\theta),\sigma_f) \tag{3}$$

Therefore,

$$p\left(\hat{f}_i|\theta,\mathcal{M}\right) = \left(2\pi\sigma_f^2\right)^{-\frac{1}{2}} \exp\left(-\frac{1}{2}\left(\frac{\hat{f}_i - f_i(\theta)}{\sigma_f}\right)^2\right) \tag{4}$$

Similarly, the same reasoning can be adopted to get the likelihood of mode component $p\left(\hat{\phi}_i|\theta,\mathcal{M}\right)$, but this would lead to the well-known 'mode matching problem' [34]. In order to avoid this, a novel discrepancy function is proposed that makes use of the well-known MAC criterion [35], as $J_\phi(\theta) = 1 - \mathrm{MAC}_i(\theta) \in [0,1]$, with $\mathrm{MAC}_i(\theta)$ as

$$\mathrm{MAC}_i(\theta) = \frac{|\langle\hat{\phi}_i, \phi_i(\theta)\rangle|}{\|\hat{\phi}_i\|^2 \|\phi_i(\theta)\|^2} \tag{5}$$

where $\langle\cdot,\cdot\rangle$ is the Euclidean inner product between the two vectors and $\|\cdot\|$ is the Euclidean norm. Since θ is uncertain, J_ϕ is a non-negative uncertain value and the maximum entropy distribution for a non-negative unbounded variable is the log-normal distribution, therefore

$$p(\hat{\phi}_i|\theta,\mathcal{M}) = \left(2\pi s^2\right)^{-\frac{1}{2}} J_\phi(\theta)^{-1} \exp\left(-\frac{1}{2s^2}\left(\log\frac{J_\phi(\theta)}{x_0}\right)^2\right) \tag{6}$$

with x_0 and s as the log-normal scale and dispersion parameters, respectively. The last equation can be used to compute the likelihood function using Eq. (2), however a simplified version could be easily obtained by assuming moderately high values for the dispersion parameter s and $x_0 \approx 1$, leading to a close to zero value for the argument of the exponential function in Eq. (6), and therefore

$$p(\hat{\phi}_i|\theta, \mathcal{M}) \approx \left(2\pi s^2\right)^{-\frac{1}{2}} \frac{1}{1 - \mathrm{MAC}_i(\theta)} \quad (7)$$

After some pilot runs, the influence of the dispersion parameter s on the model updating results was revealed as negligible, thus it can be assumed as constant. Therefore, $p(\hat{\phi}_i|\theta, \mathcal{M}) \propto (1 - \mathrm{MAC}_i(\theta))^{-1}$, and, according to the Metropolis–Hastings algorithm adopted in this work (refer to Section 3.2.3), there is no need to fix such a constant since it vanishes in Eq. (8).

3.2.3. BIP solution by using stochastic simulation

The Metropolis–Hastings (M–H) algorithm [36,37] is adopted as a stochastic simulation to obtain the posterior distribution, $p(\theta|\mathcal{D}, \mathcal{M})$ (Eq. (1)). This algorithm is versatile and easy to implement and generates samples from a specially constructed Markov chain whose stationary distribution is the posterior PDF $p(\theta|\mathcal{D}, \mathcal{M})$. By sampling a candidate parameter $\boldsymbol{\theta}'$ from a *proposal distribution* $q(\boldsymbol{\theta}'|\boldsymbol{\theta}^{\zeta})$, the M–H obtains the state of the chain at $\zeta+1$, given the state at ζ, specified by $\boldsymbol{\theta}^{\zeta}$. Candidate parameter $\boldsymbol{\theta}'$ is accepted (i.e., $\boldsymbol{\theta}^{\zeta+1} = \boldsymbol{\theta}'$) with probability $\min\{1, r\}$, and rejected (i.e., $\boldsymbol{\theta}^{\zeta+1} = \boldsymbol{\theta}^{\zeta}$) with the remaining probability $1 - \min\{1, r\}$, where:

$$r = \frac{p(\mathcal{D}|\boldsymbol{\theta}', \mathcal{M}) p(\boldsymbol{\theta}'|\mathcal{M}) q(\boldsymbol{\theta}^{\zeta}|\boldsymbol{\theta}')}{p(\mathcal{D}|\boldsymbol{\theta}^{\zeta}, \mathcal{M}) p(\boldsymbol{\theta}^{\zeta}|\mathcal{M}) q(\boldsymbol{\theta}'|\boldsymbol{\theta}^{\zeta})} \quad (8)$$

The process is repeated until N_s samples have been generated so that the monitored acceptance rate (ratio between accepted M–H samples over the total amount of samples) reaches asymptotic behaviour. During such updating process, no manual intervention nor pre-calibration of parameters is needed. A pseudo-code description of this method is provided below as Algorithm 1.

Algorithm 1: M–H algorithm

Initialize $\boldsymbol{\theta}^{\zeta=0}$ by sampling from the prior PDF: $\boldsymbol{\theta}^0 \sim p(\boldsymbol{\theta}|\mathcal{M})$;
for $\zeta = 1$ **to** N_s **do**
  Sample from the proposal: $\boldsymbol{\theta}' \sim q(\boldsymbol{\theta}'|\boldsymbol{\theta}^{\zeta-1})$;
  Compute r from Eq. (8);
  Generate a uniform random number: $\alpha \sim \mathcal{U}[0, 1]$;
  if $r \geqslant \alpha$ **then**
    Set $\boldsymbol{\theta}^{\zeta} = \boldsymbol{\theta}'$;
  else
    Set $\boldsymbol{\theta}^{\zeta} = \boldsymbol{\theta}^{\zeta-1}$;
  end
end

The described methodology is embedded within a parameterised computational framework by coupling the Bayesian algorithms and the FE model simulations (refer to Fig. 4), which enables the Bayesian learning process to be fully automated.

4. Real case study

The methodology for updating structural FE models proposed in this paper is illustrated here for a sixteenth century cultural heritage building in Granada (Spain), the San Jerónimo Monastery.

4.1. Ambient vibration tests

The Ambient Vibration Tests (AVTs) are carried out to identify the natural frequencies, the modal shapes and the modal damping of the building. Fig. 5 shows a schematic representation of the sensor layout. The configuration consists of a total of 62 points to be measured. All measurement points are tracked in the three main directions, in order to capture global vibration modes. Since eight triaxial accelerometers are available for the testing process and two of them are kept fixed as reference points, a series of 12 measurements is necessary to cover all the measurement points. In each of these sets, accelerations are recorded with a sampling frequency of 100 Hz and a sampling time of 12 min.

Excitations during ambient vibration tests are associated with environmental loads. The used equipment consists of force-balanced accelerometers with dimensions of 13.3 cm in diameter and 6.2 cm in height (model ES-T). The equipment has a bandwidth ranging from 0.01 to 200 Hz, a dynamic range of 155 dB, and a recording range of ±0.25 g to ±4 g. These accelerometers are connected, via five 40 m cables and three 100 m long cables, to a 36-channel data acquisition system with a 24-bit ADC, provided with anti-alias filters (OBSIDIAN X36, ROCK+, GRANITE model). Fig. 6 shows the experimental campaign.

Table 1
Results OMA: Natural frequencies (f), damping coefficients (ϵ), and MAC values.

	SSI		EFDD		MAC
	f (Hz)	ϵ (%)	f(Hz)	ϵ (%)	
Mode 1	1.01	1.28	1.01	0.59	0.96
Mode 2	1.38	1.11	1.38	0.9	0.99
Mode 3	1.85	2.00	1.85	0.96	0.96
Mode 4	2.42	2.74	2.39	0.58	0.7

4.2. Operational modal analysis

The measurements recorded by the accelerograms in the AVT (Section 4.1) are processed by two Operational Modal Analysis (OMA) methods: (i) Stochastic Subspace Identification (SSI) [38], and (ii) Enhanced Frequency Domain Decomposition (EFDD) [39] in the frequency domain. Both methods are implemented using Artemis software, and the natural frequencies (f), damping coefficients (ϵ), and modal shapes obtained are subsequently correlated using the Modal Assurance Criterion (MAC) in order to assess the accuracy of the mode shapes obtained (see Table 1).

As Table 1 shows, the ambient vibration tests allows the first four vibration modes in a range of frequencies up to 2.42 Hz to be accurately identified. Regarding the mode shapes, the MAC values are higher than 0.96 for the first three modes, indicating good correlation between both methods (SSI and EFDD).

Fig. 7 shows the first four mode shapes obtained from OMA. As can be observed, the first mode is the only one that can be considered local since it only affects the tower through a bending with respect to the YZ plane, the second identified mode corresponds to the combination of a bending of the tower in the XZ plane and a transverse translation mode in the transept area in the ZY plane. The following two modes are mainly translational in the XY horizontal plane. The third mode contemplates a simple transverse translation with a maximum displacement in the middle of the central nave in the y-direction, on the other hand, the transept shows a movement in the x-direction. The fourth mode presents a transverse translation with an inflection point half of the central nave, in addition the tower presents a twist with respect to the vertical z-axis.

The free vibration of the simplified FE model (Fig. 3), which includes soil–structure interaction, has been studied. The input model parameters are selected from a previous research work of this building [40] and 25 modes of vibration are calculated. Most of the modes are related to mechanical simplifications, do not correspond to the real structure, and they have not a relevant weight of the effective mass. Table 2 summarises the effective mass of the modes which are related to the real structure:

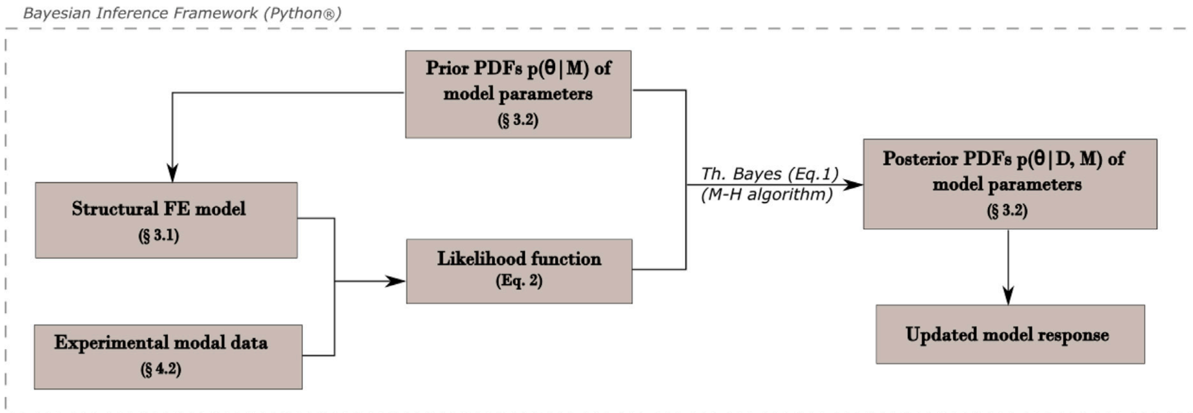

Fig. 4. Parameterised computational model of the Bayesian Inference.

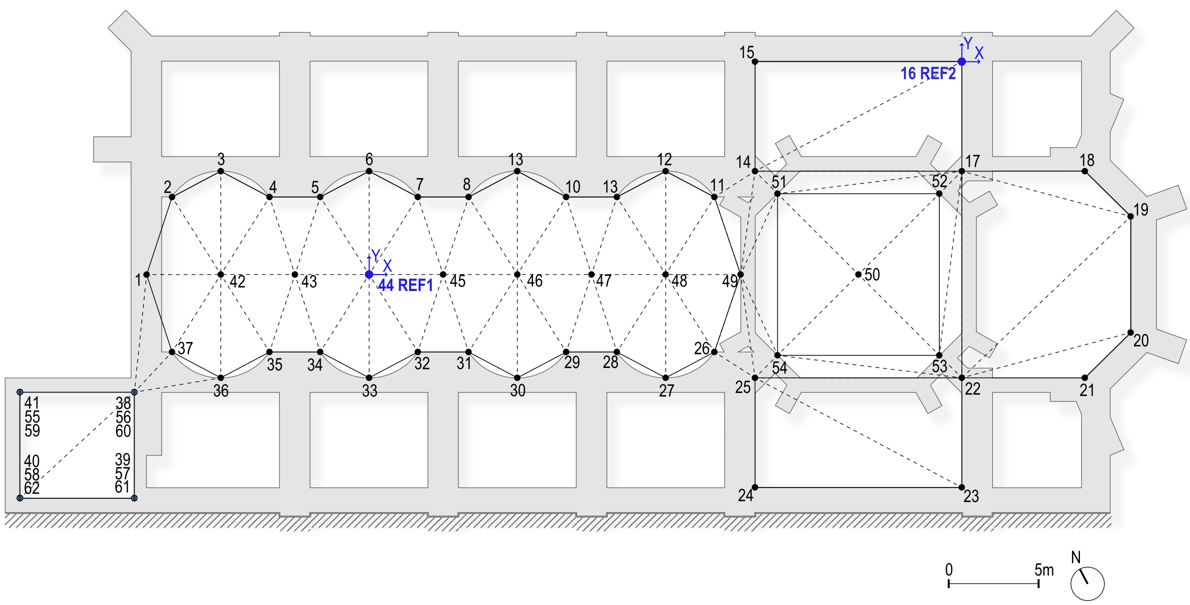

Fig. 5. Accelerometer locations directions. In the central church, accelerometers are located on top of the cannon. In the tower (shown in the left) measurements were taken at different altitudes.

Table 2
Effective mass of the vibration modes.

	f (Hz)	Effective mass (%)		
		x-direction	y-direction	z-direction
Mode 1	1.05	68.61	2.67	3.07
Mode 2	1.5	7.90	5.89	89.70
Mode 3	1.92	0.004	43.24	0.41
Mode 4	2.01	10.54	11.67	6.00
Mode 5	2.52	10.91	20.65	0.09
Mode 6	2.72	0.33	14.97	0.57

As evident from the effective mass analysis, the response of the structure is mainly governed by the first two modes of vibration. These two modes provide the largest effective mass in the x-direction and z-direction. The third mode, responsible of the largest effective mass in the y-direction, is mainly due to the movement of the soil. Therefore, in this work the first two natural frequencies and mode shapes estimated from the OMA are taken as the reference data set for the model updating procedure using the Bayesian approach.

4.3. Bayesian model parameters identification

The FE modelling described in Section 3.1 is parameterised considering the bulk modulus of the main construction material (E), the main cloister walls (E_c), the one of the inner arcade of the church (E_a), and the stiffness of the soil (k), as uncertain input model parameters. The prior distributions of these input model parameters, $\mathcal{D} = \{E, k, E_c, E_a, \sigma_f\}$, are represented by uniform distributions and are summarised in Table 3. In particular, the range of values for the bulk modulus of the stone (E) and the main cloister (E_c) have been fixed according to a previous research work of the limestone (calcarenite) of Granada [20]. The stiffness of the soil (k) is in reasonable agreement with the approximated values for the modulus of subgrade reaction proposed by Bowles [41]. Finally, the bulk modulus of the arcade (E_a) it is within the range of values expected for handmade bricks [21,22], its actual construction material.

Then, samples from the posterior PDFs of the model parameters are obtained using the M–H algorithm with 150,000 realisations. The prior, posterior $p(\theta|\mathcal{D}, \mathcal{M})$ and the maximum a *posteriori* (MAP) of each individual parameter ($\theta_1 = E$, $\theta_2 = k$, $\theta_3 = E_c$, $\theta_4 = E_a$, $\theta_5 = \sigma_f$) are represented in Fig. 8. Note that the identified MAP values of the model parameters are consistent with the physical reality.

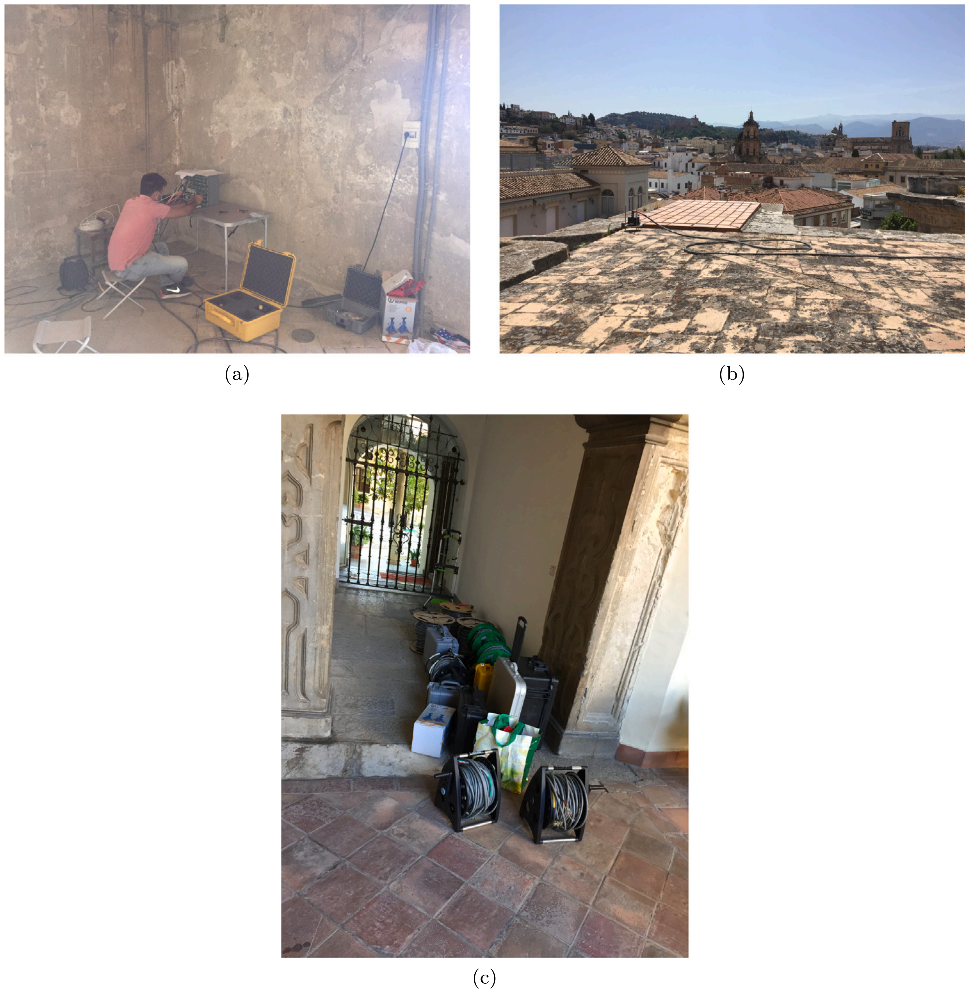

Fig. 6. Experimental campaign of the Ambient Vibration Tests (AVTs).

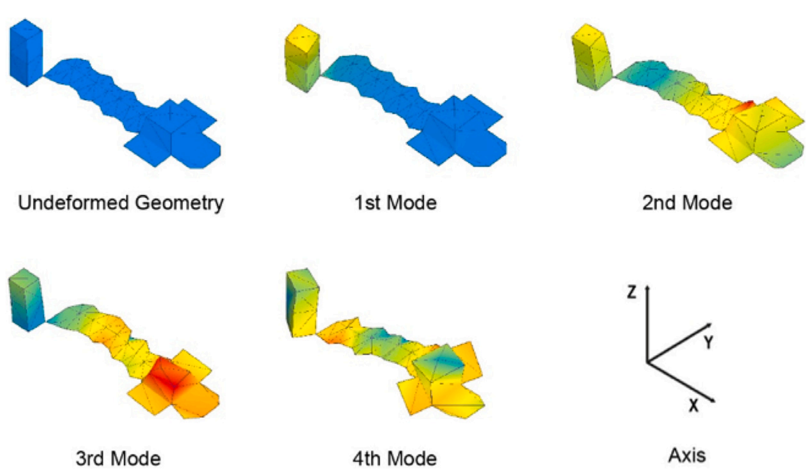

Fig. 7. The first four mode shapes obtained from OMA.

Table 3
Prior information of model parameters.

	$\theta_1 = E$ [MPa]	$\theta_2 = k$ [N/m]	$\theta_3 = E_c$ [MPa]	$\theta_4 = E_a$ [MPa]	$\theta_5 = \sigma_f$
$p(\boldsymbol{\theta}\mid\mathcal{M})$	$\mathcal{U}(0.35, 2) \cdot 10^4$	$\mathcal{U}(1.5, 8.5) \cdot 10^6$	$\mathcal{U}(0.35, 2) \cdot 10^4$	$\mathcal{U}(0.7, 4.2) \cdot 10^3$	$\mathcal{U}(1.2, 7.5) \cdot 10^{-2}$

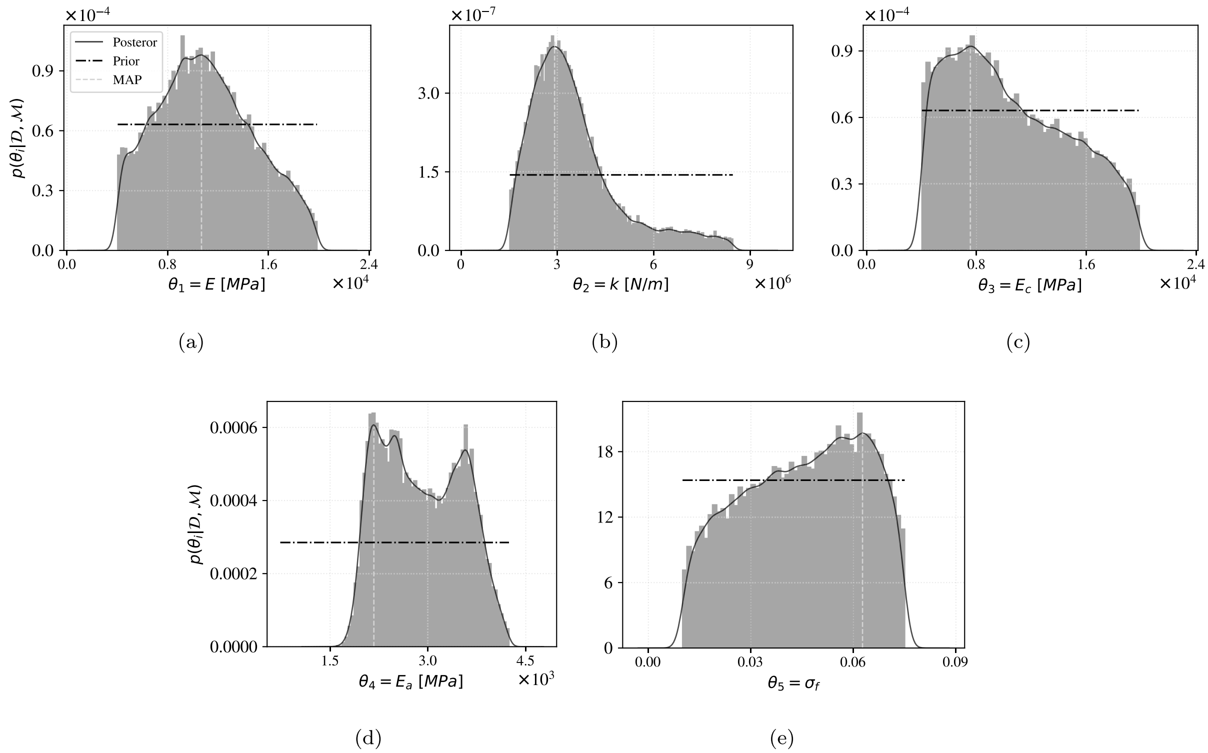

Fig. 8. Priors (black dashed line), posterior (solid line), and maximum a *posteriori* (grey dashed line) of the input parameters: (a) bulk modulus of the stone E, (b) soil stiffness k (c) bulk modulus of the cloister E_c, (d) bulk modulus of the arcade E_a, (e) uncertain parameter σ_f.

Also note that parameters learn from data as there is a clear information shrinkage, from non-informative uniform priors to concentrated probability density function. However, the posterior uncertainty in the model parameters identification is relatively high, meaning that there is an irreducible discrepancy between the modelled and experimental responses. If a more detailed FEM model is used, such uncertainty will be reduced.

Finally, in order to check the validity of the parameters identification problem, the FE model is simulated using the posterior samples of the model parameters, and the first two frequencies and modes are computed. Fig. 9 shows the probability density functions for the simulated frequencies in comparison with measured ones (Fig. 9. a–b), and results for the simulated MAC values (Fig. 9. c–d). It can be observed that the frequency response of the model using the posterior PDF parameters is accurate (its MAP values are very close to the frequencies measured) and its level of uncertainty is relatively low. MAC values, present moderately high MAP values (0.6 for f_1 and 0.65 for f_2), and higher uncertainty. This also responds to an irreducible discrepancy between the simulated and measured shape modes.

5. Discussion

A Bayesian methodology for parameter identification from ambient vibration tests in CH buildings has been presented in this paper. The proposed methodology is generic and as such, it can be applied to any other structure providing on availability of AVTs data. Here it has been specialised to a particular CH stone masonry building, for which a series of assumptions have been made. The implications of some of these modelling assumptions as well as the lessons learned from this research are discussed here for the sake of clarity and greater extensibility.

First, this study has considered a limited amount of uncertain model parameters to be updated, namely, the most sensitive ones after a Global Sensitivity Analysis. The reason is twofold: (1) considering all possible uncertain parameters would lead to a significant increase of the 'unnecessary' model complexity in relation to the data, thus biasing the inference results [8]. It means that the model will not generalise well when making predictions since it depends too much of the details of the data (even noise). This observation contradicts the general 'forward problem' conception that more complex analysis may be necessary to capture the minor details of the complex reality. For inverse problems, such as the model parameter updating presented here, this may not be the case. Simpler models should be preferred over more complex models that lead to only slightly better agreement with the data. This is an instance of the well-known Principle of Model Parsimony or *Ockham's razor* [8]. The other reason (2) is the high computational cost associated to such an (unnecessary) high-dimensional model updating process, which, in addition to the computational complexity of the FE model, would make the updating process unfeasible in practice, requiring high performance computation.

Second, a simplified FE model of the CH building has been adopted in this research in order to substantially reduce the computational complexity of the overall model updating process. This FE model relies on the assumptions that the building material properties (e.g., the bulk modulus of stone) remain the same throughout the entire building, and that some internal building structures such as the inner arcade of the church and the main cloister walls can be represented by springs elements whose stiffnesses are then identified in the model updating process, among others. Such simplifying assumptions will have an impact on the uncertainty of the posterior PDFs of the model parameters, as shown in Fig. 8, so that the harder the assumption the more spread out the PDFs of the model parameters. If a more detailed FE model was adopted, such as the underlying soil below [42], a less uncertain parameter identification would have been obtained; however, this is at the cost of heavy computation. In this sense, computational techniques such as HPC computing or surrogate modelling would be required to substantially reduce the overall computational cost so that the proposed Bayesian updating methodology can be feasible in real life buildings such as the investigated here.

Finally, it is important to remark that for the case study presented here, the first two natural frequencies and mode shapes were used

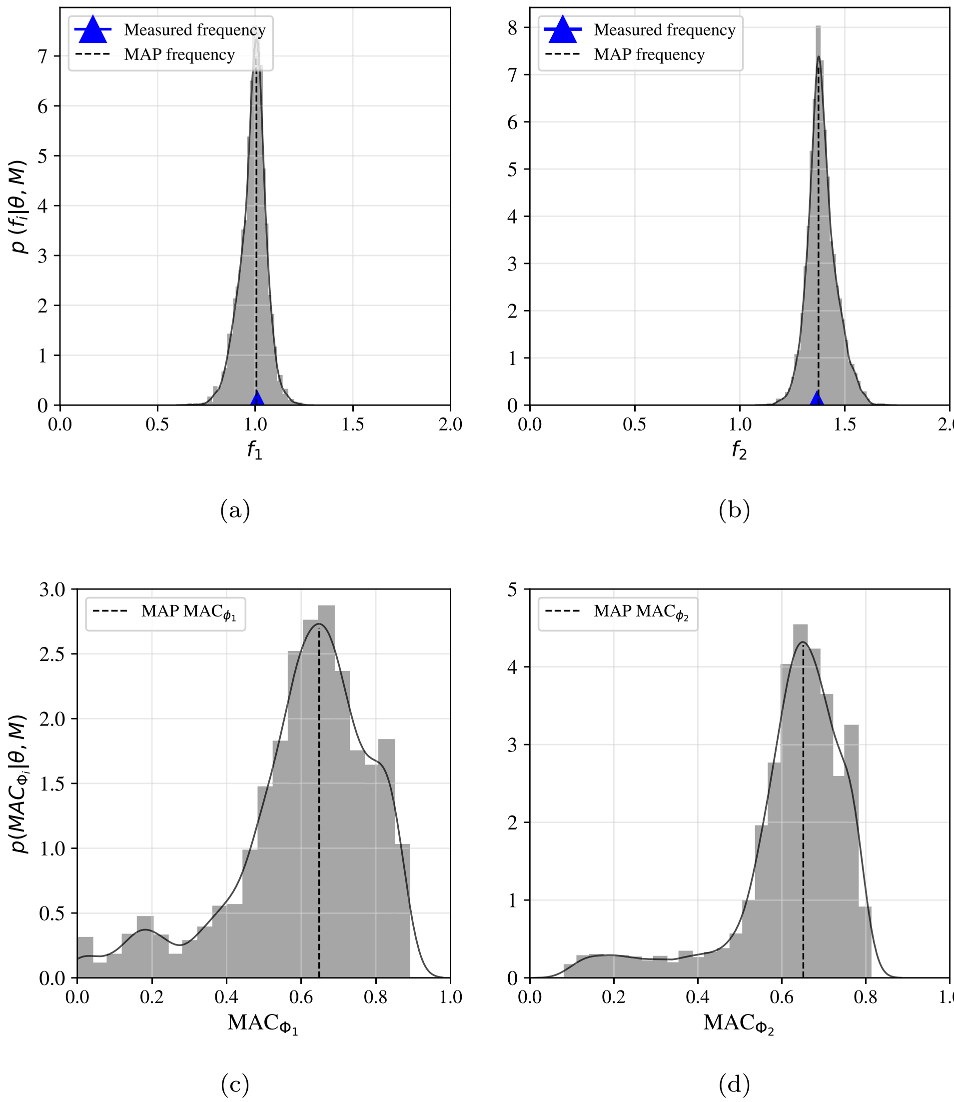

Fig. 9. Maximum a posteriori (dashed line), measured frequency (blue triangle) and simulated values (solid line) of: (a) modelled f_1 frequency, (b) modelled f_2 frequency, (c) modelled MAC of the f_1 frequency, (d) modelled MAC of the f_2 frequency. (For interpretation of the references to colour in this figure legend, the reader is referred to the web version of this article.)

as input data for the Bayesian updating process. These were revealed as the most relevant ones after an effective mass analysis, shown in Table 2. The consideration of less relevant modes in the parameter identification process would have ended in higher uncertainty following the Principle of Model Parsimony discussed before. In any case, the adoption of more or less vibration modes is case specific and does not invalidate the proposed methodology.

6. Conclusions

A Bayesian learning methodology has been presented in this paper to infer the most plausible values of the material and structural parameters of a cultural heritage building based on modal information from ambient vibration data. The suitability and effectiveness of the method have been tested in real case study, the San Jerónimo Monastery, a sixteenth century CH building in Granada (Spain). As evident from the results, the methodology allows several sources of uncertainty to be accounted for in the inference process, such as the uncertainty coming from the measurements noise and the epistemic uncertainty coming from the adoption of a 3D macro-modelling approach to represent the modal response of the entire building. Besides, the following conclusions and lessons learned are drawn from this paper:

- The Bayesian learning paradigm presented in this manuscript has shown efficiency in identifying the uncertain model parameters in a real large-scale CH building. However, this efficiency was gained by adopting several modelling simplifying assumptions which translated into larger posterior uncertainty. This suggests a trade-off between model precision and uncertainty that is inherent in the Bayesian learning process and needs to be assessed in a case specific basis.
- For a given FE model of the building, selecting a parsimonious amount of updatable model parameters will prevent increasing the unnecessary model complexity. Such an unnecessary complexity may lead to biased inference results.
- After a pilot run using frequencies as the only system output, the additional consideration of the modal shapes was revealed as key for a more robust parameter identification. The incorporation of the MAC values in a soundly probabilistic way within the Bayesian learning methodology is regarded as the main methodological novelty of the paper.

Further research work is under consideration with regards to the adoption of more detailed large-scale FE models of the entire building including the material non-linearities within the proposed framework at a reasonable computational cost. This requires the adoption of meta-modelling techniques or high performance computation in such a way that the resulting updating framework can be executed in quasi-real time in a continuous Structural Health Monitoring context.

CRediT authorship contribution statement

Enrique Hernández-Montes: Conceptualization, Supervision, Funding acquisition. **María L. Jalón:** Software, Writing – original draft, Writing – review & editing. **Rubén Rodríguez-Romero:** Ambient vibration tests, Operational modal analysis. **Juan Chiachío:** Conceptualization, Methodology, Formal analysis, Supervision, writing – review. **Víctor Compán-Cardiel:** Ambient vibration tests, Operational modal analysis. **Luisa María Gil-Martín:** Software (FE modelling), Supervision.

Declaration of competing interest

The authors declare that they have no known competing financial interests or personal relationships that could have appeared to influence the work reported in this paper.

Data availability

No data was used for the research described in the article.

Acknowledgements

This work is part of the HYPERION project (https://www.hyperion-project.eu/). HYPERION has received funding from the European Union's Framework Programme for Research and Innovation (Horizon 2020) under grant agreement no. 821054. The content of this publication is the sole responsibility of UGR and does not necessarily reflect the opinion of the European Union. Furthermore, the authors would like to thank Dr M. Alejandro Fernandez-Ruiz (University of Cádiz, Spain) for providing computer access to ANSYS, and to University of Granada/CBUA for funding for open access charge.

References

[1] Rus G, Chiachío J, Chiachío M. Logical inference for inverse problems. Inverse Probl Sci Eng 2016;24(3):448–64.
[2] Torres W, Almazán JL, Sandoval C, Boroschek R. Operational modal analysis and FE model updating of the Metropolitan Cathedral of Santiago, Chile. Eng Struct 2017;143:169–88.
[3] Clementi F, Pierdicca A, Formisano A, Catinari F, Lenci S. Numerical model upgrading of a historical masonry building damaged during the 2016 Italian earthquakes: The case study of the Podestà palace in Montelupone (Italy). J Civ Struct Health Monit 2017;7(5):703–17.
[4] Formisano A, Krstevska L, Lorenzo GD, Landolfo R, Tashkov L. Experimental ambient vibration tests and numerical investigation on the Sidoni Palace in Castelnuovo of San Pio (L'Aquila, Italy). Int J Mason Res Innov 2018;3(3):269–94.
[5] Standoli G, Giordano E, Milani G, Clementi F. Model updating of historical belfries based on OMA identification techniques. Int J Archit Herit 2021;15(1):132–56.
[6] Standoli G, Salachoris GP, Masciotta MG, Clementi F. Modal-based FE model updating via genetic algorithms: Exploiting artificial intelligence to build realistic numerical models of historical structures. Constr Build Mater 2021;303:124393.
[7] Ashayeri I, Biglari M, Formisano A, D'Amato M. Ambient vibration testing and empirical relation for natural period of historical mosques. Case study of eight mosques in Kermanshah, Iran. Constr Build Mater 2021;289:123191.
[8] Beck JL. Bayesian system identification based on probability logic. Struct Control Health Monit 2010;17(7):825–47.
[9] Chiachío-Ruano J, Chiachío-Ruano M, Sankararaman S. Bayesian Inverse Problems: Fundamentals and Engineering Applications. CRC Press; 2021.
[10] Cheung SH, Bansal S. A new Gibbs sampling based algorithm for Bayesian model updating with incomplete complex modal data. Mech Syst Signal Process 2017;92:156–72.
[11] Jang J, Smyth A. Bayesian model updating of a full-scale finite element model with sensitivity-based clustering. Struct Control Health Monit 2017;24(11):e2004.
[12] Pepi C, Gioffre M, Grigoriu M. Bayesian inference for parameters estimation using experimental data. Probab Eng Mech 2020;60:103025.
[13] Lam H-F, Yang J, Au S-K. Bayesian model updating of a coupled-slab system using field test data utilizing an enhanced Markov chain Monte Carlo simulation algorithm. Eng Struct 2015;102:144–55.
[14] Ierimonti L, Venanzi I, Cavalagli N, Comodini F, Ubertini F. An innovative continuous Bayesian model updating method for base-isolated RC buildings using vibration monitoring data. Mech Syst Signal Process 2020;139:106600.
[15] Akhlaghi MM, Bose S, Mohammadi ME, Moaveni B, Stavridis A, Wood RL. Post-earthquake damage identification of an RC school building in Nepal using ambient vibration and point cloud data. Eng Struct 2021;227:111413.
[16] Liu P, Huang S, Song M, Yang W. Bayesian model updating of a twin-tower Masonry structure through subset simulation optimization using ambient vibration data. J Civ Struct Health Monit 2021;11(1):129–48.
[17] Atamturktur S, Hemez F, Laman J. Uncertainty quantification in model verification and validation as applied to large scale historic Masonry monuments. Eng Struct 2012;43:221–34.
[18] Monchetti S, Viscardi C, Betti M, Bartoli G. Bayesian-based model updating using natural frequency data for historic masonry towers. Probab Eng Mech 2022;70:103337.
[19] Luque A, Cultrone GV, Sebastián Pardo E, Cazalla Vázquez O, et al. Evaluación de la eficacia de tratamientos en el incremento de la durabilidad de una calcarenita bioclástica (Granada, España). Materiales de Construcción 2008;58(292):115–28.
[20] Gil-Martín LM, Fernández-Ruiz MA, Hernández-Montes E. Mechanical Characterization and Creep Behavior of a Stone Heritage Material Used in Granada (Spain): Santa Pudia Calcarenite. Rock Mech Rock Eng 2022;55(9):5659–69.
[21] Pérez-Gálvez F, Rodríguez-Liñán C, Rubio P. Determinación de las características mecánicas de los muros de fábrica de ladrillo en la arquitectura doméstica sevillana de los siglos XVIII y XIX. Inform de la Construcción 2009;61(514):19–28.
[22] Ferreyra Hirschi E, Rocco C, Eperjesi L. Evaluación de la resistencia mecánica de muros de mampostería de ladrillos. Jornada de Técnicas de Restauración Y Conservación Del Patrimonio 1. 2009.
[23] Menéndez E, Martín LG, Salem Y, Jalón L, Hernández-Montes E, Alonso M. Bayesian assessment of surface recession patterns in brick buildings with critical factors identification. Boletín de la Sociedad Española de Cerámica Y Vidrio 2022.
[24] RIEGEL Laser Measurement Systems. 2010, http://www.riegl.com/products/terrestrial-scanning/produktdetail/product/scanner/4/ [Accessed: 30 Sept 2010].
[25] Agisoft L. Agisoft photoscan pro. Russia: St. Petersburg; 2014, Available Online At: http://www.agisoft.com.
[26] Milani G, Shehu R, Valente M. Possibilities and limitations of innovative retrofitting for Masonry churches: Advanced computations on three case studies. Constr Build Mater 2017;147:239–63.
[27] Valente M, Milani G. Seismic response and damage patterns of Masonry churches: Seven case studies in Ferrara, Italy. Eng Struct 2018;177:809–35.
[28] Yacila J, Camata G, Salsavilca J, Tarque N. Pushover analysis of confined masonry walls using a 3D macro-modelling approach. Eng Struct 2019;201:109731.
[29] Valente M. Seismic vulnerability assessment and earthquake response of slender historical masonry bell towers in South-East Lombardia. Eng Fail Anal 2021;129:105656.
[30] Zhang Z, Huang M, Xu C, Jiang Y, Wang W. Simplified solution for tunnel-soil-pile interaction in Pasternak's foundation model. Tunnel Undergr Space Technol 2018;78:146–58.
[31] Murin J, Aminbaghai M, Kutis V, Hrabovsky J. Modal analysis of the FGM beams with effect of axial force under longitudinal variable elastic Winkler foundation. Eng Struct 2013;49:234–47.
[32] Saltelli A, Ratto M, Andres T, Campolongo F, Cariboni J, Gatelli D, et al. Global sensitivity analysis: the primer. John Wiley & Sons; 2008.
[33] Jaynes ET. Information theory and statistical mechanics. Phys Rev 1957;106(4):620.
[34] Yuen K-V. Bayesian methods for structural dynamics and civil engineering. John Wiley & Sons; 2010.
[35] Allemang RJ. A correlation coefficient for modal vector analysis. In: Proc. 1st int. modal analysis conference. 1982, p. 110–6.
[36] Metropolis N, Rosenbluth AW, Rosenbluth MN, Teller AH, Teller E. Equation of state calculations by fast computing machines. J Chem Phys 1953;21(6):1087–92.
[37] Hastings WK. Monte Carlo Sampling Methods Using Markov Chains and Their Applications. Biometrika 1970;57(1):97–109.
[38] Brincker R, Ventura CE, Andersen P. Damping estimation by frequency domain decomposition. In: Proceedings of IMAC 19: a conference on structural dynamics. Society for Experimental Mechanics; 2001, p. 698–703.
[39] Van Overschee P, De Moor B. Subspace identification for linear systems: Theory-Implementation-Applications. Springer Science & Business Media; 2012.
[40] Jalón ML, Chiachio J, Gil-Martín LM, Chiachío M, Rodríguez-Romero R, Compán-Cardiel V, et al. Updating structural FE models of cultural heritage assets based on probabilistic tools. In: Proceedings of the 31th european safety and reliability conference. published by research publishing, singapore. 2021.
[41] Bowles JE. Foundation analysis and design. 1988.
[42] De Angelis A, Lourenço PB, Sica S, Pecce MR. Influence of the ground on the structural identification of a bell-tower by ambient vibration testing. Soil Dyn Earthq Eng 2022;155:107102.